

Depinning Transition in Type-II Superconductors

N. Lütke-Entrup, B. Plaçais, P. Mathieu, and Y. Simon

Laboratoire de Physique de la Matière Condensée de l'Ecole Normale Supérieure CNRS URA 1437,
24 rue Lhomond, F-75231 Paris Cedex 5, France

(Received 30 April 1997)

The surface impedance $Z(f)$ of conventional isotropic materials has been carefully measured for frequencies f ranging from 1 kHz to 3 MHz, allowing a detailed investigation of the depinning transition. Our results exhibit the irrelevance of classical ideas to the dynamics of vortex pinning. We propose a new picture, where the linear ac response is entirely governed by disordered boundary conditions of a rough surface, whereas in the bulk vortices respond freely. The universal law for $Z(f)$ thus predicted is in remarkable agreement with experiment, and tentatively applies to microwave data in YBaCuO films. [S0031-9007(97)04152-5]

PACS numbers: 74.60.Ge, 74.25.Nf

A perfect sample of a type-II superconductor in the vortex (or mixed) state would be transparent to an electromagnetic wave at very low frequencies. But defects are always present and strongly alter the quasistatic and low-frequency response; low frequencies here means $\Omega = 2\pi f \ll \Omega_d$, a so-called “depinning frequency” [1] depending on the material and vortex density. It is important for applications to know what kind of defects can pin vortices, how they hinder small vortex oscillations and thereby restrain the penetration of an ac ripple. In this respect, a study at low levels of excitation of both the resistive and inductive part of the surface impedance $Z(\Omega) = R - iX$ as a function of the frequency provides much information about the dynamics of pinning. It is generally accepted that bulk pinning centers limit the quasistatic skin effect to a pinning (or Campbell's) length $\lambda_C \sim 1-100 \mu\text{m}$, while dissipation is vanishingly small, as observed [1,2]. No model, however, has been able to account for variations of Z at higher frequencies. In particular, as the first increasing of $R(f)$ is stronger than expected, the understanding of dissipation remains a puzzling problem, including in high T_c materials [3].

Experiments are performed on a series of slabs of cold-rolled polycrystalline PbIn and pure single-crystalline Nb. The slabs (xy) are immersed in a normal magnetic field \mathbf{B} ; unless specified their thickness $2d$ is much larger than the flux-flow penetration depth δ_f (see below). At equilibrium, up to the upper critical field B_{c2} , a regular lattice of vortex lines parallel to z is formed, with the density $n = B/\varphi_0$, where φ_0 is the flux quantum. Both faces of the slab, $z = \pm d$, are then subjected to an ac magnetic field $b_0 e^{-i\Omega t}$ parallel to the length (x direction) of the sample. Under such conditions, induced currents and electric fields, $J(z)$ and $e(z)e^{-i\Omega t}$, are along the y direction, while vortices oscillate in the x - z planes. For low exciting fields ($b_0 \sim 1 \mu\text{T}$), vortex displacements $u(z) \sim 1 \text{ \AA}$ are very small compared with the vortex spacing $a \approx n^{-\frac{1}{2}}$ ($\sim 1000 \text{ \AA}$, for $B \sim 0.1 \text{ T}$) [Fig. 1(a)]. The electric field e_0 at the surface $z = d$, $e_0 = e(d) = -e(-d)$, is mea-

sured by means of a pick-up wound coil. The main experimental difficulty in such measurements is to ensure a precise calibration of the phase φ of e_0 (within better than 0.5° at 100 kHz). Thus we get the surface impedance of the slab, defined as the ratio $\mu_0 e_0/b_0$. Putting

$$\frac{iZ}{\mu_0 \Omega} = \frac{ie_0}{\Omega b_0} = \lambda^* = \lambda' + i\lambda'' = \Lambda e^{i\varphi}, \quad (1)$$

the ac response will be conveniently expressed in terms of the complex penetration length λ^* [4]. As is easily seen, $2b_0\Lambda$ (a factor of 2 for two faces) represents the amplitude of the ac magnetic flux penetrating the slab per unit length along y . The length λ'' measures the dissipation, as $\lambda''/\Lambda = R/|Z|$ is the sine of the loss angle φ .

The analysis of the ideal response, though it is not observed (unless $\Omega \gg \Omega_d$), is an important step in our

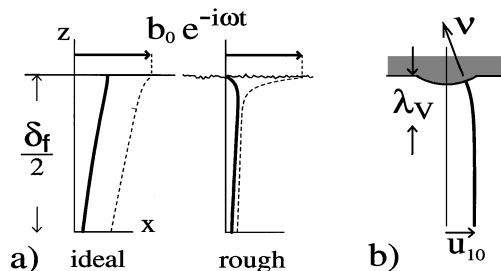


FIG. 1. (a) Vortex lines $u(z)$ (full lines), and field profiles $b(z)$ (dashed lines) near one face of a thick slab are sketched with arbitrary units; for clarity, the actual length scaling, $u \ll a \ll \delta_f$, is not preserved. For an ideal surface, vortices end normal to the plane boundary, the weight of the k_2 mode [11] is lowered, and a large normal-like skin effect is observed. For a real rough surface, a vortex-slippage effect at the surface induces a relatively strong bending of vortices over the depth $\lambda_V \sim a$, so that nondissipative currents associated with this vortex curvature [9,10] are greatly screening the exciting field. (b) An isolated superfluid vortex in a rotating box of helium II terminates at a wall asperity. If it is acted on in the bulk, the vortex line bends near the wall so as to keep on ending normal to the surface, making thus an angle with the mean smooth surface.

argument. A perfect slab would behave like a linear continuous medium, of resistivity ρ_f and permeability $\mu = \mu_r \mu_0$ ($0 < \mu_r < 1$). Here $\rho_f \approx \rho_n B/B_{c2}$ is the flux-flow resistivity, and μ is the effective ‘‘diamagnetic permeability’’ of the mixed state [5,6]; μ_r increases steadily with the vortex density and rapidly approaches unity (typically $\mu_r > 0.9$ for $B \gtrsim 0.2B_{c2}$ in PbIn). In the absence of pinning, an electromagnetic wave, $b \propto e^{\pm ik_1 z} e^{-i\Omega t}$, $e = \mp \Omega b/k_1$, can propagate in the bulk, according to the simple equation of dispersion $k_1^2 = i\mu\Omega/\rho_f = 2i/\delta_f^2$ [4]. The wave field $b(z)$ would be accordingly: $b_{10} \cosh(ik_1 z)/\cosh(ik_1 d)$, where $b_{10} = \mu_r b_0$ if one makes allowance for a surface screening by diamagnetic currents. This leads to $\lambda_{\text{ideal}}^* = \mu_r \lambda_f \tanh(d/\lambda_f)$, where $\lambda_f = (1+i)\delta_f/2$. Assuming $\mu_r \approx 1$, this (undisputed) result involves all features of a normal skin effect. In the so-defined *thick limit* (thick slabs and/or high frequencies), say $d \gtrsim 2\delta_f$, $\lambda_{\text{ideal}}^* = \mu_r \lambda_f \approx \lambda_f$, so that $\lambda' = \lambda'' = \delta_f/2$. In the *thin limit*, say $d \lesssim \delta_f$, $\lambda_{\text{ideal}}^* = \mu_r d \approx d$, which means perfect transparency.

As shown in Fig. 2, the actual response is quite different: after a low-frequency plateau, $\lambda^* \approx \lambda'(0)$ ($\lambda'' \approx 0$, $\varphi \approx 0$), the loss angle increases with frequency, so that the ideal skin effect ($\lambda^* \approx \lambda_f$, $\varphi = \pi/4$) is recovered beyond some depinning frequency Ω_d ; this can be precisely defined as the midfrequency for which $\varphi = \pi/8$. Note, in passing, that the observation of a linear response is not consistent with predictions of a naive critical state model: A critical-current density as small as $J_c \sim 10$ A/cm² should restrict the penetration

of fields $b_0 \sim 1$ μ T to depths $\Lambda = b_0/\mu_0 J_c \lesssim 1$ μ m, which is much smaller than observed, and seeing that $\Lambda \propto b_0$, no linear regime could exist at all. The linear skin effect over depths $\Lambda \sim 100$ μ m was first reported by Alais and Simon [7], and then misinterpreted by considering the possibility of thermally activated vortex motion. Soon after, Campbell suggested that the linear signal was due to small reversible oscillations of vortices in their pinning potential wells [2]: if a pinning restoring force $-nKu$ (per unit volume) is introduced in the equation of vortex motion, the propagation of the k_1 mode is greatly altered. At low frequencies, it becomes a nondissipative evanescent mode decaying exponentially in the sample over a small depth $\lambda_C = (B\varphi_0/\mu_0 K)^{1/2} \sim 1$ –100 μ m. Here $\Omega_d = \rho_f K/B\varphi_0$ [$\delta_f(\Omega_d) = \lambda_C \sqrt{2}$, $\varphi = \pi/8$] [1]. Assuming $\mu_r \approx 1$ and $\lambda_C \ll d$, the Campbell expression for λ^* reads

$$-k_1^2 = \frac{1}{\lambda^{*2}} = \frac{1}{\lambda_f^2} + \frac{1}{\lambda_C^2} \quad (d \gtrsim 2\lambda_C). \quad (2)$$

With $\lambda_f^2 = i\delta_f^2/2$, Eq. (2) accounts for the low-frequency plateau and the related order of magnitude of Ω_d . Otherwise, no satisfactory fits of both $\lambda'(\Omega)$ and $\lambda''(\Omega)$ can be obtained from Eq. (2), as shown in Figs. 2 and 3. In spite of recent attempts to improve the treatment of bulk pinning, the same difficulties are encountered in fitting $R(f)$ in YBaCuO [3]. Note in this respect that the inclusion of thermal flux-creep effects [4] may enhance the dissipation in an intermediate range of frequencies, as required (Fig. 4); it should be emphasized, however, that

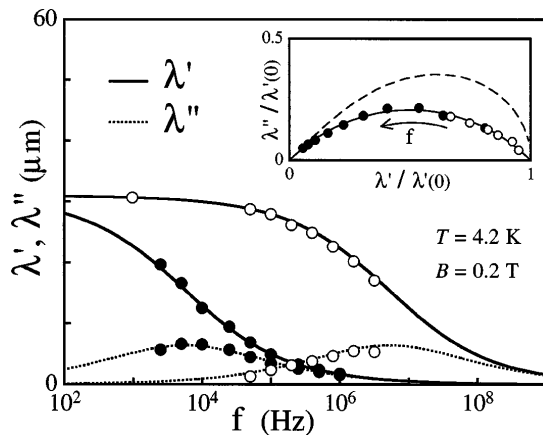


FIG. 2. The frequency dependence of the effective penetration depth $\lambda^* = \lambda' + i\lambda''$ in the thick limit ($d \gtrsim 2\delta_f$). Experimental data: (O) Pb_{0.82}In_{0.18} ($2d = 1.26$ mm, $\rho_f = 4.8$ $\mu\Omega$ cm, $\Omega_d/2\pi = 6$ MHz). (●) pure niobium ($2d = 0.85$ mm, $\rho_f = 4.3$ n Ω cm, $\Omega_d/2\pi = 6$ kHz). Full lines are theoretical fits using Eq. (5), where λ_s is the only adjustable parameter; the flux-flow resistivity ρ_f (then δ_f or λ_f) is measured from the dc voltage-current characteristics. According to Eq. (5) the universal Argand diagram of $\lambda^*(f)/\lambda^*(0)$ is the quarter circle shown in the inset: $[1 + (\Omega/\Omega_d)e^{-i\pi/4}]^{-1}$. For comparison the dashed line is the diagram predicted by the Campbell equation (2).

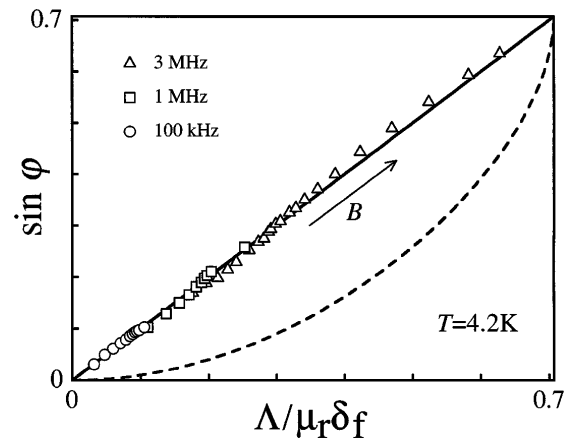


FIG. 3. The complex penetration depth $\lambda^* = \Lambda e^{i\varphi}$ of the PbIn slab referred to in Fig. 2 has been measured as a function of the magnetic field B , for three values of the driving frequency. Experimental data are plotted as the sine of the loss angle φ as function of the ratio $\Lambda/\mu_r \delta_f$, so as to verify the relation $\Lambda = \mu_r \delta_f(\Omega, B) \sin \varphi$ (straight line) resulting from Eq. (5). The limit $\sin \varphi = 1/\sqrt{2}$ corresponds to the normal state or to the depinned vortex array. The Campbell equation (2) leads to much smaller loss angles: $\Lambda^2 = \frac{1}{2}\delta_f^2 \sin 2\varphi$ (dashed line).

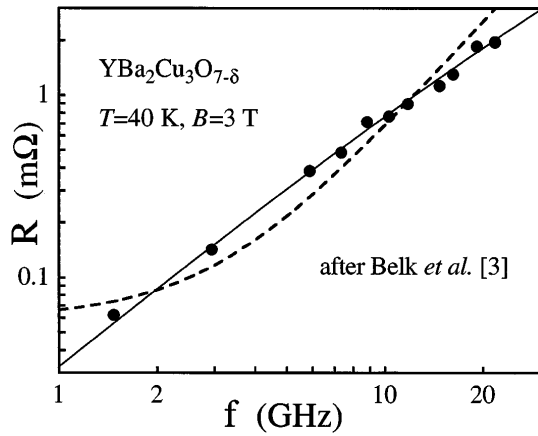


FIG. 4. The microwave surface resistance R of an YBaCuO film (sample No. 2 of Ref. [3]) vs frequency plotted in a log-log scale. (●) are experimental data taken from Fig. 6 of Ref. [3]. The full line is a fit using our Eq. (5), and taking λ_s and ρ_f (or λ_f) as two adjustable parameters (we find $\lambda_s = 0.07 \mu\text{m}$, $\rho_f = 0.4 \mu\Omega \text{cm}$, $\Omega_d/2\pi = 100 \text{GHz}$). This fit is very close to the empirical power law $R \sim f^{1.27}$ proposed by the authors. The dashed line shows the best fit obtained in Ref. [3] from the Coffey-Clem flux creep model [4].

flux-creep models [4,7] predict an unobserved divergence: $\lambda' = \lambda'' \propto \Omega^{-\frac{1}{2}}$, as $\Omega \rightarrow 0$ [8].

The model of the critical state based on the Mathieu-Simon (MS) continuum theory of the mixed state [9,10], has prompted us to an alternative interpretation. We briefly recall the points of importance in the MS theory: (i) each vortex line (unit vector $\boldsymbol{\nu}$) must terminate normal to the surface ($\boldsymbol{\nu} \times \mathbf{n} = 0$); whence the leading part of the boundary conditions (rough or smooth surface) in any problem of equilibrium or motion of vortices. (ii) Vortex lines are not always field lines, so that the vortex field $\boldsymbol{\omega} = n\varphi_0\boldsymbol{\nu}$ and the mesoscopic field \mathbf{B} must be regarded as two locally independent variables. The conjugate variable of $\boldsymbol{\omega}$, $\boldsymbol{\varepsilon} = \boldsymbol{\varepsilon}(\boldsymbol{\omega}, T)\boldsymbol{\nu}$, appears as a local line tension $\varphi_0\boldsymbol{\varepsilon}$ (J/m) in the MS equation for vortex equilibrium or nondissipative motion $\mathbf{J}_s + \text{curl}\boldsymbol{\varepsilon} = 0$. (iii) The classical picture of a local diamagnetism is misleading [6]. A diamagnetic current, just like a subcritical transport current, is a true nondissipative supercurrent $\mathbf{J}_s (= -\text{curl}\boldsymbol{\varepsilon})$ flowing near the surface over a small vortex-state penetration depth $\lambda_V (\leq \lambda_0, \text{the zero-field London depth})$. Any deviation $\boldsymbol{\omega} - \mathbf{B}$ also heals beyond the depth λ_V , so that $\boldsymbol{\omega} \equiv \mathbf{B}$ in the bulk sample. Although the mean magnetic-moment density of a perfect body turns out to be $-\boldsymbol{\varepsilon}$, the quantity $-\boldsymbol{\varepsilon}$ has not the primary physical meaning of a local magnetization, nor μ_r , conveniently defined as the ratio $\boldsymbol{\omega}/(\boldsymbol{\omega} + \mu_0\boldsymbol{\varepsilon})$, that of a true local permeability [6].

Let us return to the ac response of the slab in the standard geometry of Fig. 1, and suppose that bulk motions are unrestrained (no bulk pinning). As pointed out by Sonin *et al.* [5], the distinction between $\boldsymbol{\omega}$ and \mathbf{B} implies additional degrees of freedom, and a second k_2 mode appears besides

the classical k_1 mode ($k_1 = \pm i/\lambda_f$); this is a London-like nondispersive evanescent mode, which dies off over the depth λ_V ($k_2 = \pm i/\lambda_V$) [11]. Note that, in practice, $\lambda_V \ll \delta_f, \Lambda$ and d . In a pure k_2 -mode vortex and field lines bend in opposite directions, whereas they coincide in a pure k_1 mode. More explicitly [6,11],

$$\nu_{1x} = \frac{b_1}{B} = \frac{u_1}{\lambda_f}, \quad \nu_{2x} = -\frac{b_2}{B} \frac{\mu_r}{1 - \mu_r} = \frac{u_2}{\lambda_V}, \quad (3)$$

where $\nu_x = \partial u/\partial z$ ($\nu_{1x} = ik_1 u_{1x}$, $\nu_{2x} = ik_2 u_{2x}$) and b/B measure the slopes of vortex and field lines, respectively. Then the response $b(z)$ will be that combination of the modes, $b_1 + b_2$, which satisfies the field continuity, $b_0 = b_{10} + b_{20}$, as well as the correct boundary condition for vortex lines. The latter condition will determine the relative weights $\beta_1 = b_{10}/b_0$ and $\beta_2 = b_{20}/b_0$ of the modes ($\beta_1 + \beta_2 = 1$), and, therefore, the effective penetration depth $\lambda^* = \beta_1\lambda_f + \beta_2\lambda_V \simeq \beta_1\lambda_f$ (since $\lambda_V \ll \delta_f$ and Λ). For an ideal surface, the vortex boundary condition is clearly $\nu_x = 0$ [point (i) above]; then using Eq. (3), we just recover the simple classical-diamagnetism result, that is $\beta_1 = \mu_r$. Now, the point is that the surface roughness may considerably change this boundary condition, so as to enhance the weight of the second mode [Fig. 1(a)]. Thus we argue that small effective skin depths at low frequencies should not result from restricting the penetration of the k_1 mode, but from its amplitude being reduced due to the screening effect of the second mode.

According to the MS model [9,10,12,13], if the surface has irregularities on the scale of a , vortex lines can bend over a depth λ_V , making thus an angle α with the mean smoothed surface $z=d$. On the average, and in any direction x , α should not exceed a critical value $\alpha_c \sim 1^\circ - 10^\circ$: $\langle \nu_x \rangle_{z=d} \leq \nu_{xc} = \sin \alpha_c \sim 10^{-2} - 10^{-1}$ [9,10]. As stated above, superficial nondissipative supercurrents ($\mathbf{J}_s = -\text{curl}\boldsymbol{\varepsilon}$) can result from such distortions of the vortex array; integrating $-\text{curl}\boldsymbol{\varepsilon}$, the net current density in the y direction is $i_y (\text{A/m}) = \langle \varepsilon_x \rangle = \boldsymbol{\varepsilon} \langle \nu_x \rangle$, where $\boldsymbol{\varepsilon} \simeq B(1 - \mu_r)/\mu_r$. A dc subcritical current can be regarded as a frozen pure k_2 mode in the limit $\Omega \rightarrow 0$. To the maximum, $i_y = i_c = -\nu_{xc}B(1 - \mu_r)/\mu_r$ is the surface critical-current density. Starting from an equilibrium, where $\langle \nu_x \rangle = 0$, a shift of the bulk vortex array is expected to induce a vortex curvature in the opposite direction, $\nu_x = f(u_{\text{bulk}})$ with $\nu_{xc} = f(u \sim a)$. Perhaps such a *vortex slippage* ($\nu_x < 0$ if $u > 0$) is more intuitive when dealing with superfluid vortices in a rotating box [see Fig. 1(b)]. In helium, bulk pinning does not exist, and only asperities of the walls can pin vortices [14]. We are just extending this idea to collective motions of a vortex array along a rough surface of superconductors.

Linearizing $\nu_x = f(u_{\text{bulk}})$ for small displacements we can write $\nu_x = -u_{\text{bulk}}/l$, where l is a real length characterizing the surface roughness: $l = \infty$ would correspond

to an ideal surface; in practice we expect that $l \sim a/\nu_c \sim 0.1\text{--}10 \mu\text{m}$. As far as $\lambda_V \ll \delta_f$, this condition applies quasistatically in the ac response by taking $u_{\text{bulk}} = u_{10}$, so that the *vortex-slippage condition* reads

$$\nu_x = -\frac{u_{10}}{l}. \quad (4)$$

Now, substituting Eq. (4) for $\nu_x = 0$ in the above calculation of β_1 and β_2 , and considering the *thick limit*, we obtain

$$\frac{1}{\lambda^*} = \frac{1}{\mu_r \lambda_f} + \frac{1}{\lambda_S} \quad (\text{thick limit, } d \gtrsim 2\delta_f), \quad (5)$$

where $\lambda_S = l\mu_r/(1-\mu_r) \sim Ba/\mu_0 i_c$ is the real limit of $\lambda^* \simeq \beta_1 \lambda_f$ as $\Omega \rightarrow 0$ ($\lambda_f = \sqrt{2i} \delta_f/2$). Note that setting $\mu_r = 1$ from the beginning would lead wrongly to $\lambda^* = \lambda_f$; that is the ideal response. While giving the same low- and high-frequency limits as Eq. (2), $\lambda^*(0) = \lambda_S$ (real) and $\lambda^*(\infty) = \mu_r \lambda_f$ (depinning), Eq. (5) remarkably fits experimental data in the intermediate range $\Omega \sim \Omega_d$ (Figs. 2 and 3). According to Eq. (5), the graph $\lambda^*(\Omega)$ in the Argand diagram must be a quarter circle (Fig. 2). This universal behavior should be easily tested in any case, irrespective of any adjustable or available parameters, only providing that the thick limit is achieved.

From data taken below the thick limit (not shown in the figures), we retain an important result. When $2d$ is decreased under conditions where λ_C or $\lambda_S \ll \delta_f$ ($\Omega \ll \Omega_d$), we observe that the ac response becomes thickness dependent as soon as $d \lesssim 2\delta_f$, as predicted: just substitute $\lambda_f \tanh(d/\lambda_f)$ for λ_f in Eq. (5). In particular, the loss angle is significantly smaller than stated by Eq. (5). According to the one-mode Campbell model, size effects should arise for much thinner slabs such as $d \lesssim \lambda_C$. Note in this respect that our “pinning length” λ_S , contrary to λ_C , does not represent an actual penetration depth. The mere observation that size effects arise for $d \sim \delta_f$, not $d \sim \lambda_C$, attests that the bulk k_1 mode propagates freely, and reveals the need for a two-mode electrodynamics.

In conclusion, the MS model of the critical state completed by the vortex-slippage condition (4) accounts quantitatively for the surface impedance of a variety of conventional samples, which all have standard critical-

current densities ($i_c \sim 10 \text{ A/cm}$: polycrystalline lead-indium slabs and single-crystal slabs of pure niobium (Figs. 2 and 3). For the application to the case of YBaCuO at $f \sim 10 \text{ GHz}$, our derivation of Eq. (5) has to be reexamined, especially because of the anisotropy and high-frequency correcting terms in the dispersion equation for the two modes [11]. Nevertheless, it is worth noting that Eq. (5) may account for the observed f dependence of R in YBaCuO from 1 to 20 GHz (Fig. 4) [3]. These results support the argument, developed in previous works [9,10,12,13], that bulk pinning is absolutely ineffective in a large class of “soft” materials (devoid of strong bulk inhomogeneities). Contrary to the common idea that any crystal defect may be a pinning center, we are led to the conclusion that a normally homogeneous sample in the mixed state rather imitates the behaviour of a superfluid vortex array enclosed in a rough box.

-
- [1] J. I. Gittleman and B. Rosenblum, Phys. Rev. Lett. **16**, 734 (1966).
 - [2] A. M. Campbell, J. Phys. C **2**, 1492 (1969).
 - [3] N. Belk, D.E. Oates, D.A. Feld, G. Dresselhaus, and M. S. Dresselhaus, Phys. Rev. B **53**, 3459 (1996).
 - [4] M. W. Coffey and J.R. Clem, Phys. Rev. B **45**, 9872 (1992); **45**, 10527 (1992).
 - [5] E. B. Sonin, A.K. Tagantsev, and K.B. Traito, Phys. Rev. B **46**, 5830 (1992).
 - [6] H. Vasseur, P. Mathieu, B. Plaçaïs, and Y. Simon, Physica (Amsterdam) **279C**, 103 (1997).
 - [7] P. Alais and Y. Simon, Phys. Rev. **158**, 426 (1967).
 - [8] C. J. van der Beek, V. B. Geshkenbein, and V. M. Vinokur, Phys. Rev. B **48**, 3393 (1993).
 - [9] P. Mathieu and Y. Simon, Europhys. Lett. **5**, 67 (1988).
 - [10] T. Hocquet, P. Mathieu, and Y. Simon, Phys. Rev. B **46**, 1061 (1992).
 - [11] B. Plaçaïs, P. Mathieu, Y. Simon, E. B. Sonin, and K. B. Traito, Phys. Rev. B **54**, 13 083 (1996).
 - [12] Y. Simon, B. Plaçaïs, and P. Mathieu, Phys. Rev. B **50**, 3503 (1994).
 - [13] B. Plaçaïs, P. Mathieu, and Y. Simon, Phys. Rev. B **49**, 15 813 (1994).
 - [14] K. W. Schwarz, Phys. Rev. Lett. **47**, 251 (1981).